C. R. Mecanique 347 (2019) 576–587

Contents lists available at ScienceDirect

Comptes Rendus Mecanique

www.sciencedirect.com

Prediction of fatigue crack growth life under variable-amplitude loading using finite element analysis

Amina Remadi *, Ahmed Bahloul, Chokri Bouraoui

Mechanical Laboratory of Sousse, National Engineering School of Sousse, University of Sousse, BP 264, Erriadh, 4023 Sousse, Tunisia

ARTICLE INFO

Article history:
Received 23 April 2019
Accepted 22 June 2019
Available online 17 July 2019

Keywords:
FCG life
Memory rules
Crack-tip
Residual stress
FEA
Variable amplitude loading

ABSTRACT

This article presents an elastic-plastic study aiming at predicting the fatigue crack growth (FCG) of 2024-T3 aluminum alloys under variable-amplitude loading. The proposed analysis needs the estimation of the residual stress distribution ahead of the crack tip during propagation. An elastic-plastic FE analysis has been implemented for modeling FCG using Chaboche's model. The FE study has been carried out through consideration of the loading history effect using the memory rules. Three different loading spectra have been applied in this work. The obtained results have been compared to the experimental ones and it has been proved that the suggested model has a better prediction of the FCG lives of cracked 2024-T3 aluminum alloy structures subjected to variable-amplitude loading.

1. Introduction

The presence of cracks or discontinuities in engineering components is an inevitable phenomenon. In aerospace industry, engineers assumed the presence of cracks in aeronautical structures to ensure their safety behavior during their service lives. Therefore, the modeling of the FCG of these structures becomes a fundamental part in their design steps to prevent unexpected failure. It is well known that during service conditions, variable-amplitude loads are considered as a real loading path. In this case, FCG depends not only on the current residual stress field developed near the crack tip by the current cycle, but also on those residual stress field generated by the preceding loading history [1,2].

Various models [3–6] have been proposed to predict fatigue crack growth under variable-amplitude loading. The first category is based on the calculation of the plastic zone size ahead of the crack tip. This category was proposed firstly by Wheeler [7,8], who estimated the retardation of crack propagation due to overloads using Paris' equation multiplied by a retardation coefficient C_P. This model can predict the crack retardation caused by the application of a single and periodic overload in a spectrum of constant-amplitude loading. But it is unable to analyze the effects of underloading and those of overloads and underloads when the latter are applied together.

The second category is based on the concept of crack closure. This closure model was introduced initially by Elber [9]. He developed a relationship between the effective stress intensity factor and the crack growth rate. Then, this model is extended to predict crack growth for periodic single and block overloads and underloads [10,11]. However, the closure methodology did not take into account the load ratio effect on the threshold and it required the knowledge of the opening load.

* Corresponding author.
E-mail address: amina.remadi1@gmail.com (A. Remadi).

https://doi.org/10.1016/j.crme.2019.06.008
1631-0721/

Besides, these two categories did not take into consideration the effect of the residual stress in fatigue crack growth prediction. According to their researches, the retardation effect of FCG can be predicted using a retardation coefficient.

Later, Noroozi and Glinka [12–14] proposed a two-parameter model for FCG analysis based on the elastic-plastic response ahead the crack tip. It consists in modeling the end of the crack by a micro notch in which they assumed that the material is composed of a block of elementary size with a radius equal to the radius of the micro-notch. This model, named the "Unigrow model," is classified among the residual stress category models. The elastic-plastic stresses around the crack tips are determined using the modified Neuber method [15–18], which required the measurement of the radius of the micro-notch. Mikheevskiy et al. [19] proposed several methods to determine the elementary block size in which the choice of the appropriate method depends on the available data. Then, Correia et al. [20] have proposed a new normalized approach by adopting the cyclic J-integral to estimate the elastoplastic conditions resulting near the crack. Afterwards, Bang et al. [21] modified this model to predict FCG in the presence of a short crack.

All the previous methods have the same purpose, which is the analysis of the total fatigue life under variable-amplitude loading. However, there is no universal model.

The aim of this paper is to propose a model coupled with FE analysis able to predict the FCG live span of cracked structures subjected to variable-amplitude loading. For that, the kinematic hardening parameters for the AL2024-T3 alloy are implemented in the Abaqus software code. Comparing with experimental results, the improved model shows a good agreement in predicting fatigue life. In addition, a comparison between the proposed model and the Unigrow one is performed and analyzed.

2. Computational procedure for FCG rate under variable-amplitude loading

2.1. Two-parameter driving force model

The prediction of FCG using the two-parameter driving force model has been initially proposed by Noroozi et al. [12,13]. This model combined both the total maximum stress intensity factor SIF $k_{\max,\text{tot}}$ and the total stress intensity factor range Δk_{tot}. Thus, the FCG rate can be evaluated using the following relationship:

$$\frac{\mathrm{d}a}{\mathrm{d}N} = c\left[(k_{\max,\text{tot}})^{p}(\Delta k_{\text{tot}})^{1-p}\right]^{\gamma} \tag{1}$$

where c, p, and γ are the fitting empirical parameters of FCG data.

Later, the two-parameter driving force model has been extended to predict FCG life under random loading [14]. In fact, under the latter, the residual stress distribution has an important effect on FCG prediction and, while the stress intensity factor is defined as a driving force parameter, the residual distribution was transformed using the weight function method under the form of SIF. Then, the residual stress intensity factor k_r was added to the applied maximum stress intensity factor, $k_{\max,\text{app}}$ to obtain the total maximum stress intensity factor. Both the total maximum stress intensity factor and the total stress intensity factor range can be defined as follows [22]:

$$k_{\max,\text{tot}} = k_{\max,\text{app}} + k_\text{r} \tag{2}$$

$$\Delta k_{\text{tot}} = \Delta k_{\text{app}} \tag{3}$$

In order to estimate the residual stress intensity factor k_r, it is necessary to determine the elastic-plastic stresses/strains response of the material at the crack's area.

- **<u>Elastic stresses/strains ahead of the crack tip</u>**

The linear elastic stresses/strains ahead of the crack tip can be calculated using the Creager–Paris solution [23], expressed by the following expressions:

$$\begin{array}{ll} \sigma_{x,\max}=\frac{k_{\max}}{\sqrt{2\pi x}}\left(1-\frac{\rho}{2x}\right) & \Delta\sigma_{x,\max}=\frac{\Delta k_{\max}}{\sqrt{2\pi x}}\left(1-\frac{\rho}{2x}\right) \\ \sigma_{y,\max}=\frac{k_{\max}}{\sqrt{2\pi x}}\left(1+\frac{\rho}{2x}\right) & \Delta\sigma_{y,\max}=\frac{\Delta k_{\max}}{\sqrt{2\pi x}}\left(1+\frac{\rho}{2x}\right) \end{array} \tag{4}$$

The Creager–Paris solution was applied for a crack with a tip radius ρ. In fact, the tip radius ρ for this solution was assumed to be smaller than the crack size a ($a \gg \rho$).

- **<u>Elastic-plastic stresses/strains ahead of the crack tip</u>**

The elastic-plastic stresses/strains can be determined using the Neuber rules [15], which consist in relating the linear elastic stress/strain ($\sigma^\text{e}/\varepsilon^\text{e}$) and the actual elastic-plastic uniaxial stress/strain ($\sigma^\text{a}/\varepsilon^\text{a}$) in the crack area through the following relationships:

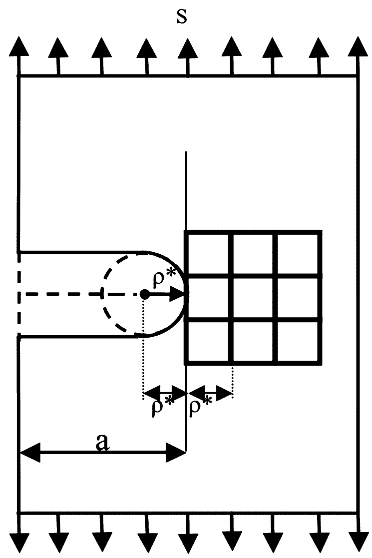

Fig. 1. Crack tip shape and elementary block size [28].

$$\sigma^{\mathrm{e}}\varepsilon^{\mathrm{e}}=\sigma^{\mathrm{a}}\varepsilon^{\mathrm{a}} \tag{5}$$

The Neuber rule has been firstly introduced in order to evaluate the elastic-plastic stress/strain for uniaxial loading, and then, it has been modified for multi-axial and variable-amplitude loading. Using the modified Neuber relationship and the Ramberg–Osgood strain/stress equation (8), the crack tip strain/stress response can be calculated as follows [24]:

$$\begin{aligned}
&\varepsilon^{\mathrm{a}}_{x,\max}=\frac{1}{E}\left(\sigma^{\mathrm{a}}_{x,\max}-\sigma^{\mathrm{a}}_{y,\max}\right)+\frac{f(\sigma^{\mathrm{a}}_{\mathrm{eq}})}{\sigma^{\mathrm{a}}_{\mathrm{eq}}}\left(\sigma^{\mathrm{a}}_{x,\max}-\frac{1}{2}\sigma^{\mathrm{a}}_{y,\max}\right)\\
&\varepsilon^{\mathrm{a}}_{y,\max}=\frac{1}{E}\left(\sigma^{\mathrm{a}}_{y,\max}-\sigma^{\mathrm{a}}_{x,\max}\right)+\frac{f(\sigma^{\mathrm{a}}_{\mathrm{eq}})}{\sigma^{\mathrm{a}}_{\mathrm{eq}}}\left(\sigma^{\mathrm{a}}_{y,\max}-\frac{1}{2}\sigma^{\mathrm{a}}_{x,\max}\right)\\
&\sigma^{\mathrm{e}}_{x,\max}\varepsilon^{\mathrm{e}}_{x,\max}=\sigma^{\mathrm{a}}_{x,\max}\varepsilon^{\mathrm{a}}_{x,\max}\\
&\sigma^{\mathrm{e}}_{y,\max}\varepsilon^{\mathrm{e}}_{y,\max}=\sigma^{\mathrm{a}}_{y,\max}\varepsilon^{\mathrm{a}}_{y,\max}
\end{aligned} \tag{6}$$

where

$$\sigma^{\mathrm{a}}_{\mathrm{eq}}=\sqrt{\left(\sigma^{\mathrm{a}}_{x,\max}\right)^2-\sigma^{\mathrm{a}}_{x,\max}\sigma^{\mathrm{a}}_{y,\max}+\left(\sigma^{a}_{y,\max}\right)^2}\quad\text{and}\quad f(\sigma^{\mathrm{a}}_{\mathrm{eq}})=\left(\frac{\sigma^{\mathrm{a}}_{\mathrm{eq}}}{k'}\right)^{\left(\frac{1}{n'}\right)} \tag{7}$$

The Ramberg–Osgood strain/stress equation is defined as follows [25]:

$$\varepsilon=\frac{\sigma}{E}+\left(\frac{\sigma}{k'}\right)^{\left(\frac{1}{n'}\right)} \tag{8}$$

where k', n' represent the cyclic hardening coefficient and exponent, respectively, and E is the modulus of elasticity.

The modified Neuber approach is based on the elementary block size ρ. In fact, it was assumed that the material is composed of identical elementary blocks of finite dimension ρ [22,26,27] and that the crack was presented as a notched with a tip radius ρ as shown in Fig. 1.

Several methods [19] have been proposed for estimating the elementary block size ρ. Noroozi et al. [13,1] developed an approach requiring the determination of the fatigue endurance limit $\Delta\sigma_{\mathrm{f}}$ and of the fatigue crack propagation threshold Δk_{th}. These two parameters can be estimated by a probabilistic S-N and FCGR model proposed by Castillo et al. [29,31] and Fernández et al. [30]. In fact, the S-N and FCGR models were applied without using any similarity or self-similarity assumptions. According to these models, ten specimens and suitable test planning would be enough to achieve a good estimation of the fatigue endurance limit [32]. This method is simple, but it is not accurate enough. In this prospect, another trial-and-error procedure was proposed [19] to determine the elementary block size ρ. This process was based on two suppositions.

- First, the fatigue crack growth was equal to the elementary block size divided by the number needed to break the distance ρ, which was determined by the following equation:

Table 1
Strain-life data Al 2024-T3 alloy [19].

σ'_f (MPa)	ε'_f	b	c
1103	0.22	−0.124	−0.59

$$\frac{\mathrm{d}a}{\mathrm{d}N} = \frac{\rho}{N} \tag{9}$$

where N is the number of cycles, which can be calculated as follows:

$$\frac{\Delta\varepsilon}{2}\sigma_{\max} = \frac{{\sigma'_{\mathrm{f}}}^2}{E}(2N)^b + \varepsilon'_{\mathrm{f}}\sigma'(2N)^c \tag{10}$$

where σ'_{f} represents the fatigue strength coefficient, $\varepsilon'_{\mathrm{f}}$ the fatigue ductility coefficient, b and c are respectively the fatigue strength exponent and the fatigue ductility exponent. Table 1 summarizes the Al 2024-T3 Strain life data.

- Second, in this method, the elementary material block size ρ was considered as a material constant that did not depend on the applied load and the specimen/crack geometry.

Nevertheless, the multi-axial Neuber's approach described above did not take into account the modification of the stress redistribution due to yielding [34]. Consequently, the residual stress distribution would not be accurately computed. Therefore, in this paper, a numerical study will be performed for the determination of the residual stress distribution near the crack tip; the latter is more realistic than the analytical solution based on Neuber's approach. More details concerning the FE analysis used in the current work are discussed in section 3.

2.2. Prediction of the residual stresses ahead of the crack tip

For variable-amplitude loading, the residual stresses ahead of the crack tip play an important role in FCG prediction. In fact, the crack growth in this case depends not only on the residual distribution generated by the current loading, but also on the residual stresses produced by the preceding loading history. In that event, the prediction of residual stresses becomes one of the most complicated parts in FCG analysis.

For that, the memory rules are combined with the finite element method to determine the residual stress ahead of the crack tip under variable-amplitude loading [12,13]. The memory model is based on three rules.

- First, it was assumed that only the compressive part of the residual stress distribution near the crack tip affects the FCG rate. These compressive residual stresses near the crack tip will be extracted using FE analysis. Then, based on the weight function method, these extracted residual stresses will be converted into SIF.
- The second rule consists in comparing the compressive part of residual stresses induced by the current loading cycle to the previous one. If the residual stresses arising from the current cycle are totally localized inside the previous one, then the current residual stresses should be neglected. If not, both residual stresses arising from the current and the previous loading cycle should be combined.
- The third rule states that when the crack reaches the compressive stresses zone, the compressive RS located in this zone must be neglected.

After the determination of the residual stresses using FE analysis coupled with the memory rules, the residual stress intensity factor $\underline{k}_{\mathrm{r}}$ can be easily computed using the following relationship:

$$k_{\mathrm{r}} = \int \sigma_r m(x,a)\mathrm{d}x \tag{11}$$

where $m(x,a)$ represents the weight function expression:

$$m(x,a) = \frac{2P}{\sqrt{2\pi(a-x)}}\left[1 + M_1\left(1-\frac{x}{a}\right)^{\frac{1}{2}} + M_2\left(1-\frac{x}{a}\right)^2 + M_3\left(1-\frac{x}{a}\right)^{3/2}\right] \tag{12}$$

The coefficients M_1, M_2 and M_3 depend on the geometry of the crack [35] and the parameter x represents the compressive residual stress zone near the crack tip.

According to several studies [36–38], these three parameters are neglected when the crack size is larger than the compressive residual stress zone. Therefore, the weight function can be expressed as follows:

$$m(x,a) = \frac{2}{\sqrt{2\pi(a-x)}} \tag{13}$$

In our study, the residual stress distribution ahead of the crack tip σ_{r} is determined using elastic-plastic finite element analysis (section 3).

Table 2
The cyclic fatigue properties and the mechanical properties for Al 2024-T3 alloy [33].

E (MPa)	ν	σ_y (MPa)	C_1 (MPa)	C_2 (MPa)	C_3 (MPa)	γ_1	γ_2	γ_3
73000	0.33	289	2169.7	7471.9	65.761	11.74	90.05	555.09

2.3. Prediction of the crack increment

Various theories [19,40,4] have been developed to determine the fatigue crack growth increment cycle by cycle. The Miner approach [41] is applied in this section. It consists of summing the current crack increment during each loading in order to obtain the total crack growth after N loads application.

$$a_N = a_0 + \sum_{i=1}^{N} \Delta a_i \tag{14}$$

where a_0 = initial crack length, Δa_i = crack increment, and a_N = total crack growth.

In this section, the determination of the fatigue crack increment induced by the current loading cycle is performed using the flowchart described in Fig. 2.

Different input parameters for this model are implemented in the first step, such as material properties, loading, geometry's specimen, crack location, initial crack size a_i, critical crack a size, ρ, FCG data: (c, γ) ... In each loading cycle, any change of these parameters can affect the prediction of the fatigue crack increment. This can be evaluated by the maximum stress intensity factor and the stress intensity range. In fact, for 'i' loading, the maximum stress intensity factor and the stress intensity range were determined as follows:

$$k_{\max,i} = \sigma_{\max,i}\sqrt{\pi a_i}\,Y \tag{15}$$

$$\Delta k_{\text{app},i} = \sigma_{\text{app},i}\sqrt{\pi a_i}\,Y \tag{16}$$

with Y evaluated as follows:

$$Y = \frac{1 - 0.5(\frac{a}{b}) + 0.32(\frac{a}{b})^2}{\sqrt{1-(\frac{a}{b})}}, \tag{17}$$

$s = \frac{P}{2bt}$ and P stands for the applied load.

The FE method is used then to estimate the residual stress distribution $\sigma_{\text{r,actual}}$ created ahead of the crack tip. This RS distribution was extracted at the end of unloading. During constant-amplitude loading, the residual stress is not modified. It remains the same. However, it propagates the crack by an increment Δa_i. Therefore, the next compressive stress will be associated with the new crack position using the memory rules to obtain $\sigma_{\text{r,result}}$ as shown in Fig. 3. Then, we calculate with the weight function the residual stress intensity factor k_{r}. The crack was considered as a 'Vierge' at the first loading cycle (without any residual stress), therefore $k_{\text{r}} = 0$ [28]. After that, we computed the total maximum stress intensity factor and the total stress intensity factor range using Eqs. (2) and (3) in order to estimate the next cracking increment.

3. FE model

In this section, the commercial finite element code ABAQUS [42] is used for FCG analysis. The specimen considered in our study (Fig. 4) is made of a 2024-T3 aluminum alloys; it exhibits a central crack size $2a = 12.7$ mm, a thickness $t = 4.1$ mm, a length $L = 610$ mm, and a width $w = 229$ mm. Chaboche's model, developed using ABAQUS software, is used to characterize the material behavior near the crack tip. The ability of this advanced model to describe the cyclic plastic deformation response ahead of the crack tip under constant- and variable-amplitude loading has been proved in several investigations [37,39,43]. Table 2 summarizes the cyclic fatigue and mechanical properties of the Al 2024-T3 alloy [33], in which C_i and γ_i represent the Chaboche kinematic hardening parameters.

In the case of variable-amplitude loading, the fatigue crack growth rate is affected, not only by the current residual stress field generated by the current cycle, but also by the residual stress fields generated by the preceding loading history. Therefore, the correct estimation of the resultant residual stress produced by all previous loading cycles should be implemented. In this context, the memory rules are used with the FE analysis to evaluate the residual stress distribution under variable-amplitude loading at the crack tip.

The finite element model for the central crack specimen is illustrated in Fig. 4, in which a boundary condition has been implemented.

For the central crack specimen, the stress intensity factor was calculated by the following expression:

$$K = S\sqrt{\pi a}\,Y \tag{18}$$

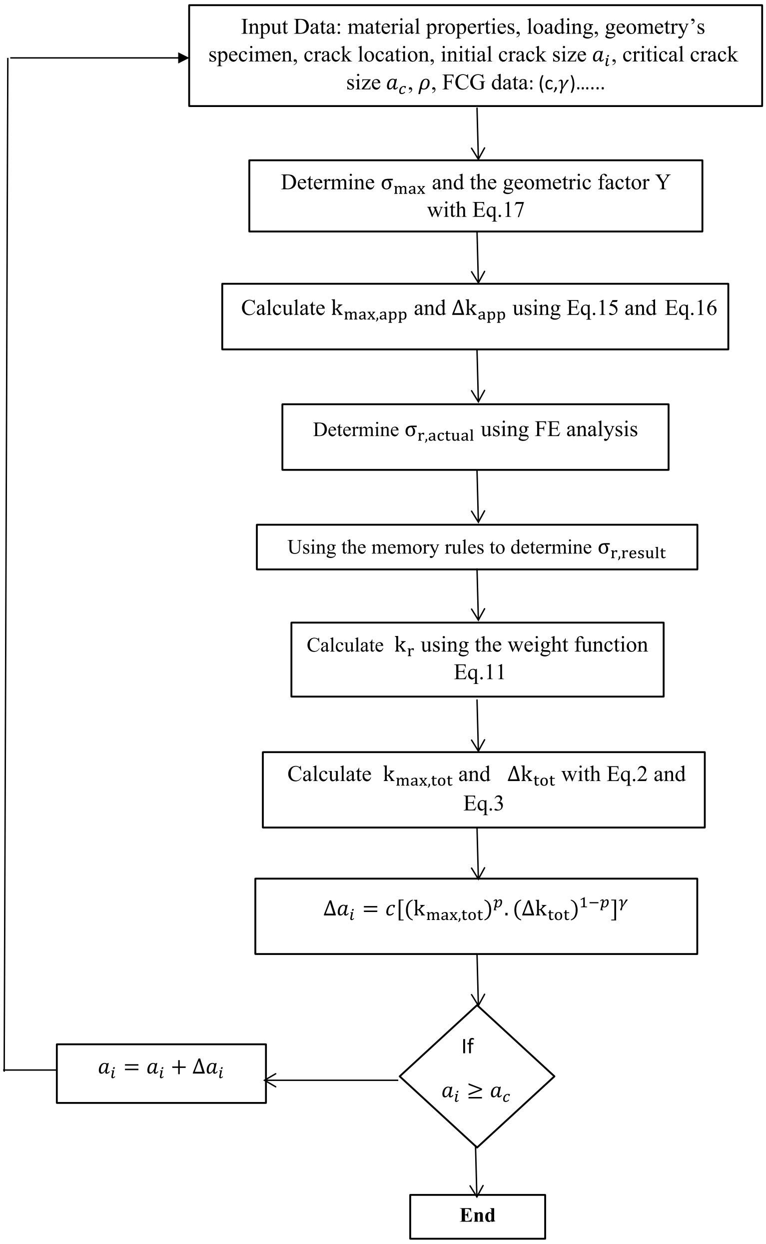

Fig. 2. Flowchart of the determination of the fatigue crack growth increment cycle by cycle.

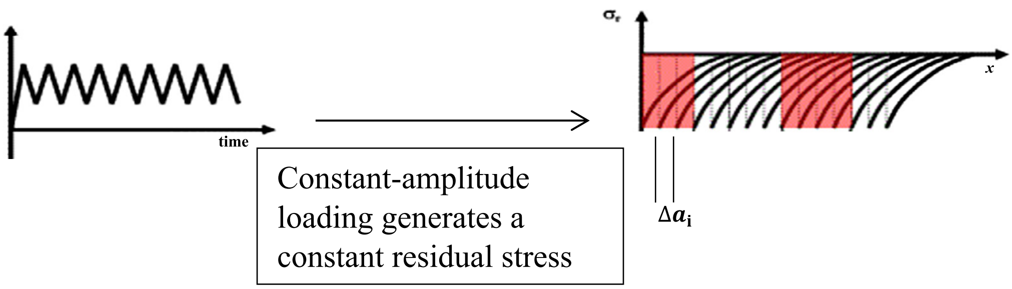

Fig. 3. Residual stress distribution for constant-amplitude loading [28].

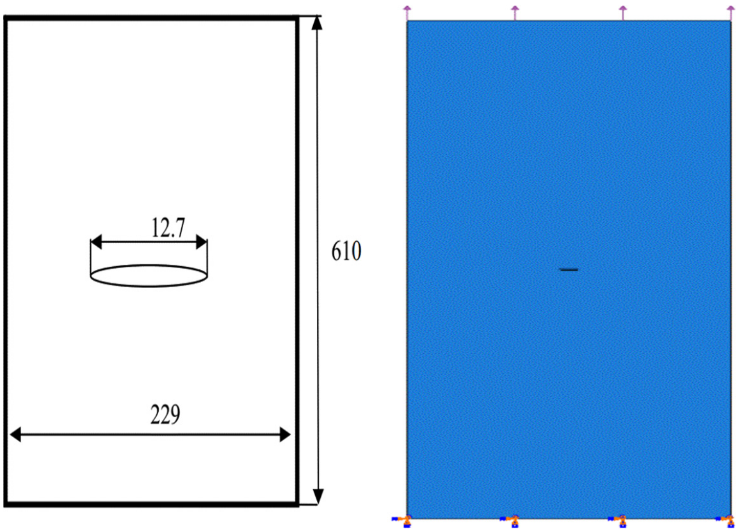

Fig. 4. Specimen dimension and boundary condition used for the simulation.

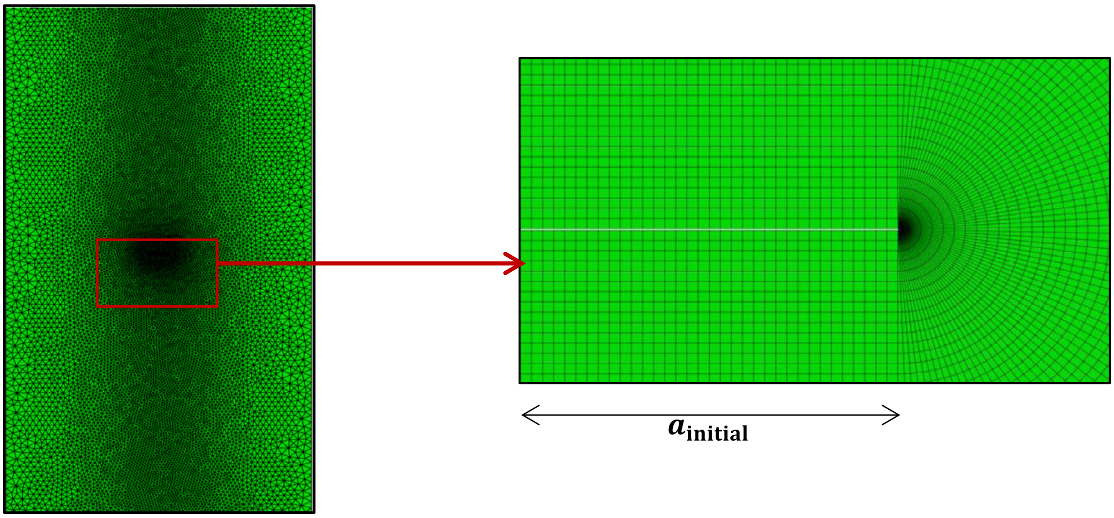

Fig. 5. Finite element mesh.

In the FE analysis, a very fine mesh has been used around the crack region with an element type CPS4R and with 0.05 elements size in order to enhance the accuracy of the FE solution in predicting the crack tip's cyclic plastic deformation response. Fig. 5 illustrates the type of mesh used.

4. Results and discussion

4.1. Prediction of the RS of the crack tip using the FE method

The crack-tip radius used for the aluminum 2024-T3 alloy according to Mikheevskiy [28] is equal to $3 \cdot 10^{-6}$ m, which is considered as the most suitable value for fatigue crack prediction. Fig. 6 presents the distribution of compressive RS near the crack tip at a maximum load value equal to 96 MPa and a stress ratio $R = 0.5$. It is shown that the maximum value of these compressive RS, in absolute value, is located in the vicinity of the crack tip. According to several studies [4,27,43], these crack tip compressive RS has a significant effect on the control of the FCG rate.

Proper prediction of FCG life under variable-amplitude loading depends on the proper estimation of these RS distributions.

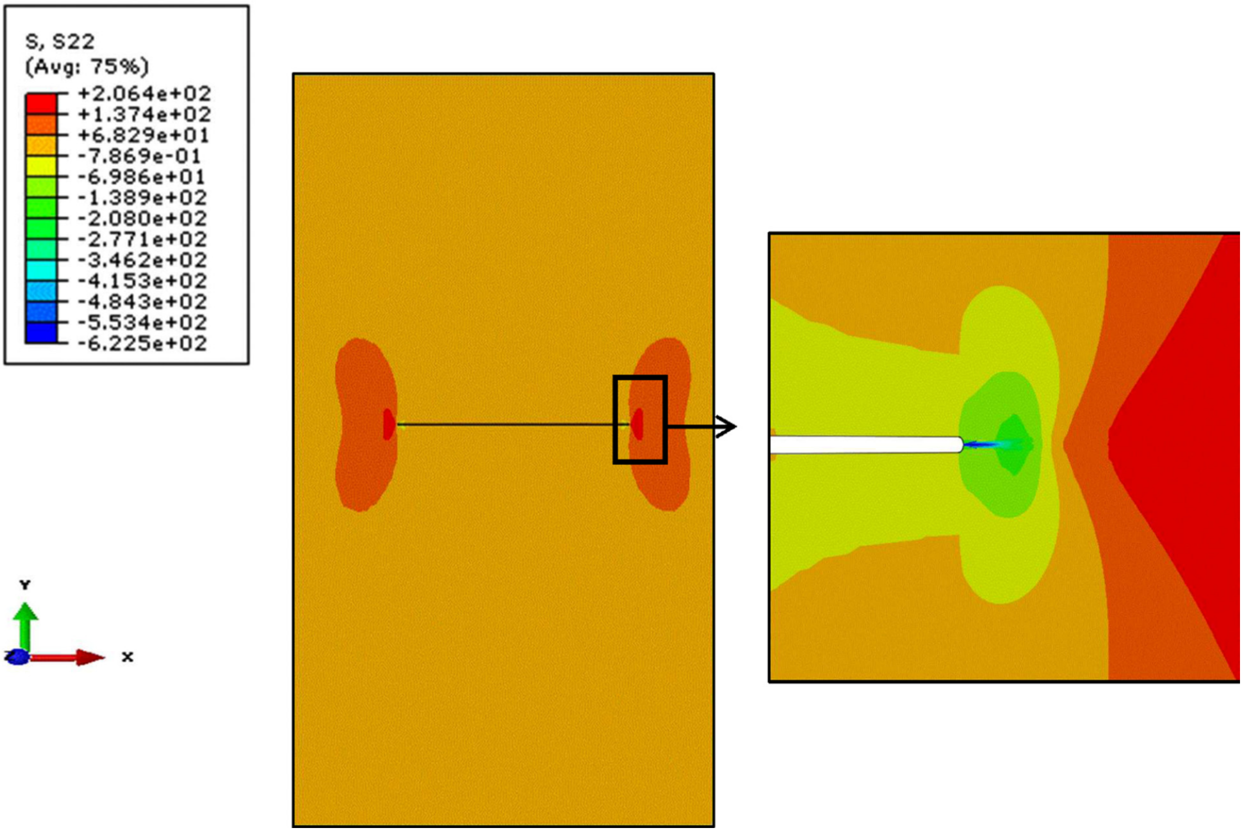

Fig. 6. Residual stress distribution ahead of the crack using FEM.

After crack extension in FE, we compared the residual stresses distribution for the current loading level with the previous ones and the memory rules was applied to estimate $\sigma_{\mathrm{r,result}}$.

4.2. Comparison between the FE method and the analytical solution

In order to assess the precision of the results of the finite element method, a comparison between the residual stresses calculated with the Neuber's method and the finite elements results for Al 2024 T3 alloy with a central crack ($2a = 12.7$ mm) was carried out (Fig. 7). In this section, we compared the numerical results with the analytical ones for two different stresses ratio equal to 0.08 and 0.5 with $\sigma_{\max}$ equal to 96 MPa.

It was observed that the compressive stress region predicted with the FE solution is smaller than the plastic zone determined with Neuber's method. There is a significant difference between the Neuber rules and the FE method. This disagreement between the two methods can be explained by the limitation of the analytical method in order to take into account the stress redistribution due to yielding [34]. In fact, the FE allows us to consider this redistribution through the extraction of the results by the path method. In addition, far from the crack region, the dispersion between the two curves becomes more important, probably due to the rapid crack growth rate.

Likewise, the determination of the residual stress distribution with the analytical method was based on the elementary block size ρ. This parameter was computed with uncertain methods. This latter is determined through methods that require the knowledge of several material parameters that are not often available.

Thus, we can conclude that the numerical method is more effective than the analytical one.

4.3. Fatigue crack growth life prediction under various loading spectra

In this analysis, three loading spectra are applied [5,28]. Fig. 8(b) pictured the first loading spectrum (high–low spectrum) with a constant stress range. In fact, the applied stress decreased from 96 MPa to 83 MPa, and then to 69 MPa. The second loading spectrum (Fig. 8(d)) is defined by a constant maximum loading (83 MPa) and a variable stress range, which was reduced from 76 MPa to 55 MPa, and then to 14 MPa. The third loading spectrum (low–high spectrum), presented in Fig. 8(f), is characterized by a constant stress range equal to 49 MPa.

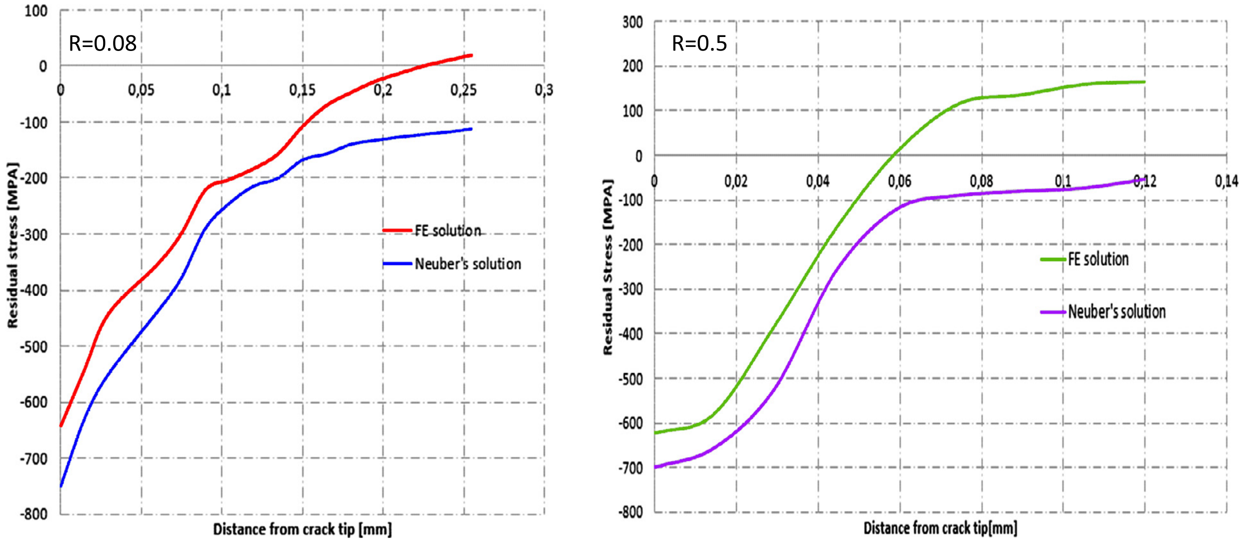

Fig. 7. Comparison of the analytical and numerical results for central crack specimens.

The aim of this paper is to validate the Chaboche kinematic hardening model (FE method), used to evaluate the residual stress distribution ahead of the crack tip. Therefore, the fatigue crack growth model described in section 2 is compared to the experimental data obtained from Refs. [5,28].

(i) A good agreement between the test data and the proposed model for the prediction of the fatigue crack growth is shown in Fig. 8(a, c, e). In fact, the fatigue crack growth using the proposed model followed in most of cases the experimental results and took into account the effect of the variation of the loading history. Besides, we can deduce that the results of our model are closer to the experimental results compared to the UNIGROW or the AFIGROW methods since, in the proposed model, we evaluated the residual stress with a reliable method (FE method).
(ii) In the case of constant maximum stress and low–high block loading, there are many dispersions of the UNIGROW and AFIGROW models compared with the experimental data in Fig. 8(c, e). This dispersion is revised in the proposed model with the determination of the residual stress by the Chaboche kinematic hardening model, embedded on the commercial FE code ABAQUS.
(iii) The results show that the variation of the stress ratio due to the changes in the block stresses (high–low or low–high) influences the prediction of fatigue crack growth. It seems that a higher stress ratio decreases the predicted number of cycles.
(iv) We can also note a that for the two-block loading (high–low) and (low–high), which are represented by a constant stress range, that the crack growth increment can be considered as a constant for different stress ratio.

5. Conclusion

The multi-axial Neuber model was the most used model to compute the residual stress ahead of the crack tip. However, this model did not take into account the modification of stress redistribution due to yielding. In this context, a numerical model combined with the memory rules has been proposed. From this work, the following conclusions can be drawn.

(1) An estimation of the compressive residual stress distribution ahead of the crack tip for variable-amplitude loading becomes more difficult than for constant-amplitude loading. This residual distribution needs to be predicted cycle by cycle while considering the previous distribution created by the previous loading. Consequently, the memory rules with the finite element method are used in this analysis.
(2) Comparison of the residual stress distribution obtained using the finite element method and the compressive residual stress computed with the multi axial Neuber method shows that the FE has a better accuracy for the fatigue crack growth prediction.
(3) The prediction of fatigue crack growth under three different loading spectra by the proposed model is in good agreement with the experimental data. Therefore, the proposed modified UNIGROW model provides a more accurate fatigue life prediction than the UNIGROW method.

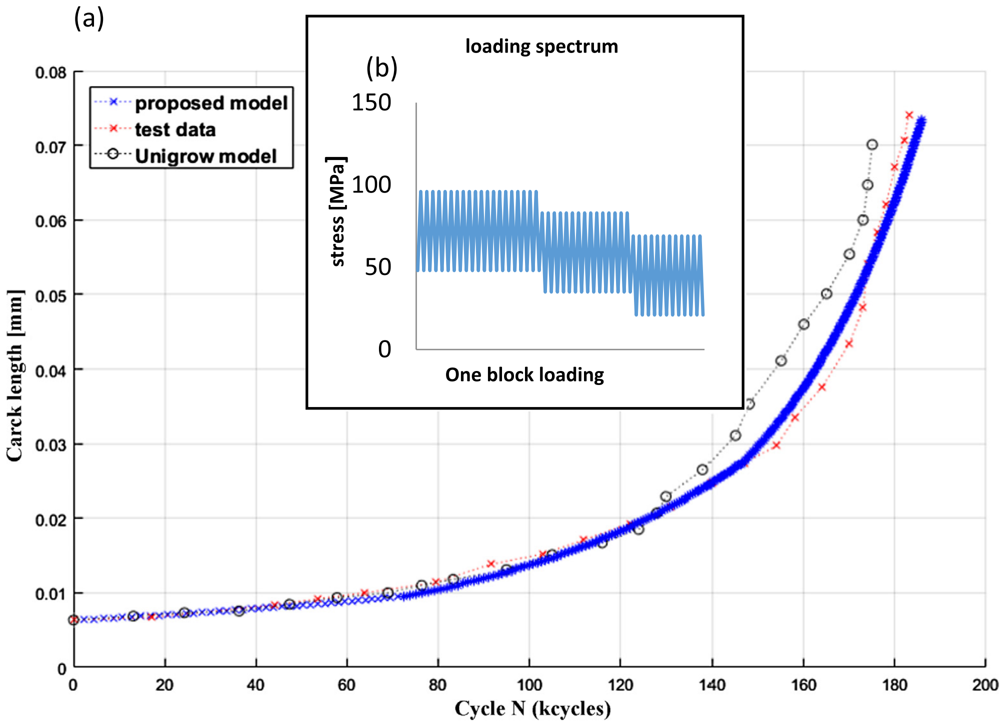

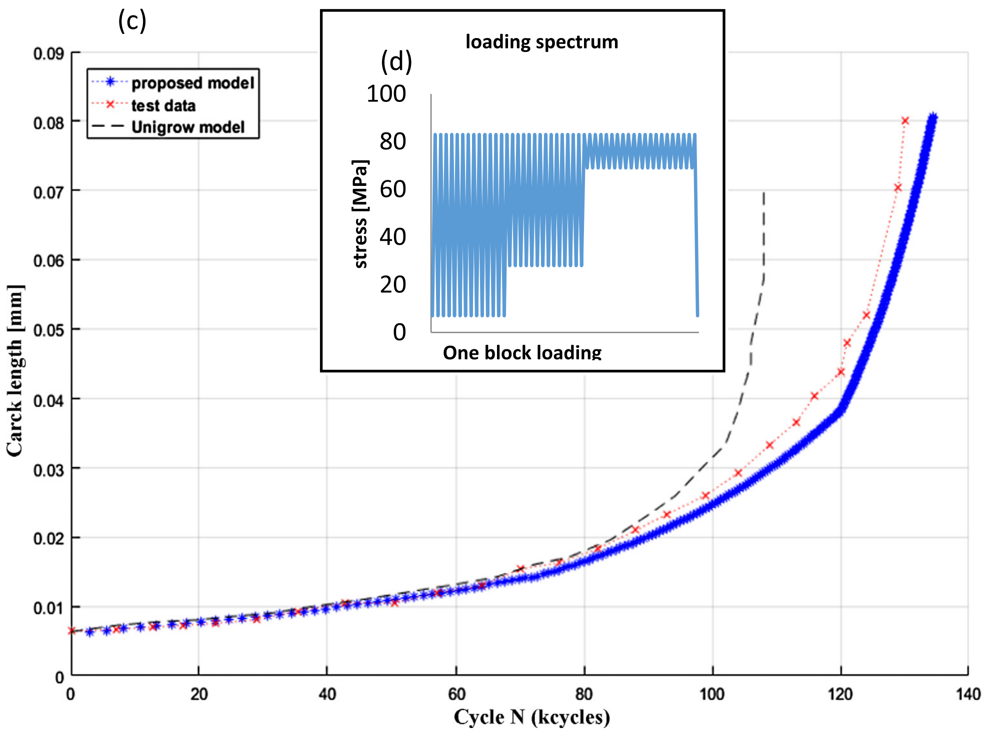

Fig. 8. Comparison of the proposed model with AL 2024-T3 experimental data [5,28] and the UNIGROW/AFIGROW model under three types of variable loading. (a) Loading spectrum. (b) Comparison of the predicted results with the experimental data. (c) Loading spectrum. (d) Comparison of the predicted results with the experimental data. (e) Loading spectrum. (f) Comparison of the predicted results with the experimental data.

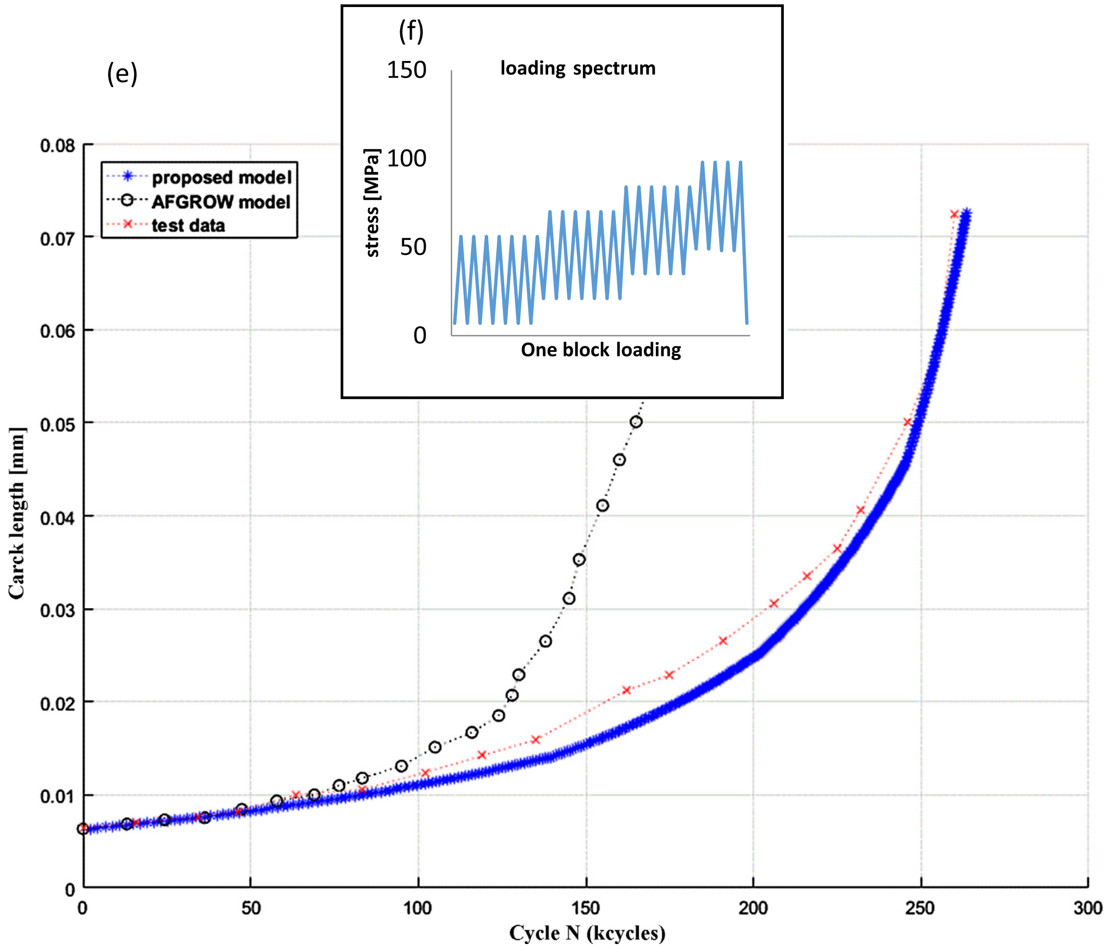

Fig. 8. (*continued*)

References

[1] A.H. Noroozi, G. Glinka, S. Lambert, A two parameter driving force for fatigue crack growth analysis, Int. J. Fatigue 27 (2005) 1277–1296.
[2] A.H. Noroozi, G. Glinka, S. Lambert, A study of the stress ratio effects on fatigue crack growth using the unified two-parameter fatigue crack growth driving force, Int. J. Fatigue 29 (2007) 1616–1633.
[3] M. Skorupa, Load interaction effects during fatigue crack growth under variable-amplitude loading – a literature review, part I: empirical trends, Fatigue Fract. Eng. Mater. Struct. 21 (1998) 987–1006.
[4] M. Skorupa, Load interaction effects during fatigue crack growth under variable-amplitude loading – a literature review, part II: qualitative interpretation, Fatigue Fract. Eng. Mater. Struct. 22 (1999) 905–926.
[5] A. Ray, R. Patankar, Fatigue crack growth under variable-amplitude loading: part II – code development and model validation, Appl. Math. Model. 25 (2001) 995–1013.
[6] A. Ray, R. Patankar, Fatigue crack growth under variable-amplitude loading: part I – model formulation in state-space setting, Appl. Math. Model. 25 (2001) 979–994.
[7] O.E. Wheeler, Spectrum loading and crack growth, J. Basic Eng. 94 (1972) 181–186.
[8] B.K.C. Yuen, F. Taheri, Proposed modifications to the Wheeler retardation model for multiple overloading fatigue life prediction, Int. J. Fatigue 28 (2006) 1803–1819.
[9] W. Elber, Fatigue crack closure under cyclic tension, Eng. Fract. Mech. 2 (1970) 35–47.
[10] A.A.A. Espinosa, N.A. Fellows, J.F. Durodola, Experimental measurement of crack opening and closure loads for 6082-T6 aluminium subjected to periodic single and block overloads and underloads, Int. J. Fatigue 47 (2013) 71–82.
[11] J. Codrington, A. Kotousov, A crack closure model of fatigue crack growth in plates of finite thickness under small-scale yielding conditions, Mech. Mater. 41 (2009) 165–173.
[12] A.H. Noroozi, Development of a Two-Parameter Model ($K_{\max}, \Delta K$) for Fatigue Crack Growth Analysis, PhD Thesis, University of Waterloo, Ontario, Canada, 2007, http://hdl.handle.net/10012/3020.
[13] A.H. Noroozi, G. Glinka, S. Lambert, A study of the stress ratio effects on fatigue crack growth using the unified two-parameter fatigue crack growth driving force, Int. J. Fatigue 29 (2007) 1616–1633.
[14] G. Glinka, A. Buczynski, Experimental and numerical analysis of elastic-plastic strains and stresses ahead of a growing fatigue crack, in: L. Susmel, et al. (Eds.), Workshop on Characterisation of Crack Tip Stress Fields, Gruppo Italiana Frattura, Forni di Sopra, Italy, 7–9 March, 2011.
[15] H. Neuber, Theory of stress concentration for shear-strained prismatical bodies with arbitrary nonlinear stress-strain law, J. Appl. Mech. 28 (1961) 544–550.
[16] A. Ince, D. Bang, Deviatoric Neuber method for stress and strain analysis at notches under multiaxial loadings, Int. J. Fatigue 102 (2017) 229–240.

[17] A. Ince, G. Glinka, A numerical method for elasto-plastic notch-root stress–strain analysis, J. Strain Anal. Eng. Des. 48 (2013) 229–244.
[18] A. Ince, G. Glinka, A. Buczynski, Computational modeling of multiaxial elasto-plastic stress–strain response for notched components under non-proportional loading, Int. J. Fatigue 62 (2014) 42–52.
[19] S. Mikheevskiy, G. Glinka, Elastic-plastic fatigue crack growth analysis under variable-amplitude loading spectra, Int. J. Fatigue 31 (2009) 1828–1836.
[20] J.A.F.O. Correia, S. Blasón, A.M.P. De Jesus, A.F. Canteli, P.M.G.P. Moreira, P.J. Tavares, Fatigue life prediction based on an equivalent initial flaw size approach and a new normalized fatigue crack growth model, Eng. Fail. Anal. 69 (2016) 15–28.
[21] D.J. Bang, A. Ince, L.Q. Tang, A modification of UniGrow 2-parameter driving force model for short fatigue crack growth, Fatigue Fract. Eng. Mater. Struct. 42 (2018) 1–16.
[22] S. Mikheevskiy, G. Glinka, D. Algera, Analysis of fatigue crack growth in an attachment lug based on the weight function technique and the UniGrow fatigue crack growth model, Int. J. Fatigue 42 (2012) 88–94.
[23] R. Baxter, N. Hastings, A. Law, E.J. Glass, Elastic field equation for blunt crack with reference to stress corrosion cracking, Int. J. Fract. Mech. 39 (2008) 561–563.
[24] T. Sciences, T. Sireteanu, I.D.M. Solidelor, Analytical method for fitting the Ramberg-Osgood model to given hysteresis loops analytical method for fitting the Ramberg-Osgood model, Proc. Rom. Acad. 15 (2014) 35–42.
[25] A.M.P. De Jesus, J.A.F.O. Correia, Critical assessment of a local strain-based fatigue crack growth model using experimental data available for the P355NL1 steel, J. Press. Vessel Technol. 135 (2012) 170–180.
[26] S. Mikheevskiy, G. Glinka, E. Lee, Fatigue crack growth analysis under spectrum loading in various environmental conditions, Metall. Mater. Trans. A, Phys. Metall. Mater. Sci. 44 (2013) 1301–1310.
[27] S. Mikheevskiy, S. Bogdanov, G. Glinka, Analysis of fatigue crack growth under spectrum loading – the UniGrow fatigue crack growth model, Theor. Appl. Fract. Mech. 79 (2015) 25–33.
[28] S. Mikheevskiy, G. Glinka, Elastic-Plastic Fatigue Crack Growth Analysis Under Variable-Amplitude Loading Spectra, University of Waterloo, Ontario, Canada, 2009.
[29] E. Castillo, A. Fernández Canteli, D. Siegele, Obtaining S–N curves from crack growth curves: an alternative to self-similarity, Int. J. Fract. 187 (2014) 159–172.
[30] A. Fernández Canteli, C. Przybilla, M. Nogal, M. López Aenlle, E. Castillo, ProFatigue: a software program for probabilistic assessment of experimental fatigue data sets, in: 17th ICMFM, Verbania, Italy, 25–27 May, Proc. Eng. 74 (2014) 236–241.
[31] E. Castillo, A. Fernández-Canteli, A Unified Statistical Methodology for Modeling Fatigue Damage, Springer, 2009.
[32] S. Blasón, A. Fernández Canteli, C. Rodríguez, Fatigue characterization of a crankshaft steel: use and interaction of new models, Frattura Integr. Strutt. 35 (2016) 524–532.
[33] T. Kebir, B. Mohamed, M. Abdelkader, Simulation of the cyclic hardening behavior of aluminum alloys simulation of the cyclic hardening behavior of aluminum alloys, Mech. Eng. 79 (2017) 240–250.
[34] Mohammad Hadi Hafezi, N. Nik Abdullah José, F.O. Correia Abílio, M.P. De Jesus, An assessment of a strain-life approach for fatigue crack growth, Int. J. Struct. Integr. 3 (2012) 344–376.
[35] G. Shen, G. Glinka, Determination of weight functions from reference stress intensity factors, Theor. Appl. Fract. Mech. 15 (1991) 237–245.
[36] P. Livieri, F. Segala, O. Ascenzi, Analytic evaluation of the difference between Oore-Burns and Irwin stress intensity factor for elliptical cracks, Acta Mech. 105 (2005) 95–105.
[37] A. Bahloul, Deterministic and Probabilistic Analysis of Fatigue Crack Growth Prediction by Crack Growth Analysis, National Engineering School of Sousse, ENISo, Sousse, Tunisia, 2017.
[38] G. Glinka, G. Shen, Universal features of weight functions for cracks in mode I, Eng. Fract. Mech. 40 (1991) 1135–1146.
[39] A. Bahloul, C.H. Bouraoui, T. Boukharouba, Prediction of fatigue life by crack growth analysis, Int. J. Adv. Manuf. Technol. (2017) 4009–4017.
[40] A.S. Ribeiro, A.P. Jesus, J.M. Costa, L.P. Borrego, J.C. Maeiro, Variable amplitude fatigue crack growth modelling, in: Proc. 8° Congresso Nacional de Mecânica Experimental – CNME, Guimarães, Portugal, 21–23 April, 2010.
[41] M.A. Miner, Cumulative damage in fatigue, J. Appl. Mech. 12 (1945) 159–164.
[42] ABAQUS/Standard User's Manual, Version 6.14.
[43] A. Bahloul, C.H. Bouraoui, The overload effect on the crack tip cyclic plastic deformation response in SA333 Gr 6 C–Mn steel, Theor. Appl. Fract. Mech. 99 (2018) 27–35.